The *Drosophila* EAST protein associates with a nuclear remnant during mitosis and constrains chromosome mobility

Martin Wasser[1],* and William Chia[2]

[1]Institute of Molecular and Cell Biology, National University of Singapore, 30 Medical Drive, Singapore 117609
[2]MRC Centre for Developmental Neurobiology, King's College London, 4th Floor, New Hunts House, Guy's Hospital Campus, London SE1 1UL, UK

*Author for correspondence (e-mail: mcbmw@imcb.nus.edu.sg)

Summary

Drosophila EAST protein associates with an interior nonchromosomal compartment of the interphase nucleus. Because overexpression of *east* can dramatically alter nuclear architecture we investigated a potential role for EAST in changing chromosome organization during the cell cycle. Following nuclear envelope breakdown, EAST remains enriched in the mitotic remnant of the interphase nucleus until the onset of anaphase. Loss of *east* expression affects the accuracy of division cycles. In female meiosis, *east* mutations lead to abnormal segregation of nonexchange chromosomes. During the syncytial nuclear cycles, increased frequency of mitotic errors leads to the depletion of surface nuclei. In the post-syncytial cell cycles, abnormal congression of chromosomes in prometaphase delays the onset of anaphase. Loss of *east* expression also results in abnormal chromosome morphology in male meiosis. We propose that EAST constitutes a component of a nucleoskeleton that helps to constrain the mobility of chromosomes in interphase, mitosis and meiosis.

Movies available online

Key words: EAST, Meiosis, Mitosis, Chromosome congression, Nucleoskeleton

Introduction

The chromosomes of the interphase nucleus are embedded into a network-like nucleoplasm, which remains structurally and functionally poorly understood. Numerous proteins, including EAST, Tpr (translocated promoter region), Plexus, CP60 and CP190, localize to this extrachromosomal nuclear domain (END) in *Drosophila* (Matakatsu et al., 1999; Oegema et al., 1997; Zimowska et al., 1997). The dramatic alterations of nuclear architecture brought about by the overexpression of the EAST protein provided new evidence that the END might contain an expandable nucleoskeleton (Wasser and Chia, 2000). The overexpression of EAST in polyploid cells resulted in the expansion of END regions between chromosomes and between chromosomes and nuclear lamina, showing that nuclear volume is determined not only by the amount of genomic DNA and the volume of the lumen of the nucleolus, but also by the extent of the lumen of the END. In addition, EAST can modulate the distribution of other proteins such as CP60 and actin inside the nucleus. These findings led us to propose that EAST might influence a putative internal nucleoskeleton (Wasser and Chia, 2000).

During the cell cycle, nuclear architecture undergoes dramatic changes as the interphase nucleus is dismantled during entry into mitosis and reassembled during exit from mitosis. During entry into mitosis, the nucleolus, nuclear envelope (NE) and lamina dissolve and their components become vesiculated (Moir et al., 2000; Olson et al., 2000). Proteins of these structures are either degraded or are recycled for the reassembly of the daughter nuclei. By contrast, other nonchromosomal proteins like CP60 and Tpr continue to be associated with a 'central nuclear remnant', even after NE breakdown, suggesting that an interior 'nuclear' structure derived from the interphase nucleus persists into mitosis (Oegema et al., 1997; Zimowska et al., 1997). A third group of proteins shuttle between the nucleus at interphase and different parts of the mitotic apparatus such as centrosomes, spindle or cleavage furrow, where they perform mitosis-specific functions. For instance, Skeletor, a nuclear protein that is associated with chromosomes during interphase, forms a spindle matrix at prophase and associates with the spindle at metaphase (Walker et al., 2000). In male meiosis, the actin binding protein Anillin localizes to the cleavage furrow and plays a role in cytokinesis (Giansanti et al., 1999).

We extended our studies on EAST by analyzing its potential role in the cell cycle. We show here that EAST is another member of a group of nonchromosomal nuclear proteins that remain associated with an internal remnant of the interphase nucleus during mitosis. Genetic studies show that *east* plays an important role in promoting the accuracy of both mitosis and meiosis. In syncytial blastoderm embryos, the removal of *east* leads to an increase in the frequency of mitotic errors and, as a result, to the elimination of surface nuclei. During mitosis in cellularized embryos, loss of *east* can delay the congression of chromosomes to the metaphase plate and consequently delay the onset of anaphase. Mutations of *east* also lead to nondisjunction of achiasmate chromosomes in female meiosis

and to abnormal chromosome morphology in male meiosis. Our results indicate that after NE breakdown, a certain structure, which includes components derived from the interphase nucleus like EAST and CP60, acts to constrain chromosome mobility and facilitates the congression of chromosomes to the metaphase plate.

Materials and Methods

Fly stocks

The *east* alleles used have been previously described (VijayRaghavan et al., 1992; Wasser and Chia, 2000). Canton-S was used as the wild-type strain. The early embryonic GAL4 driver *matalpha4-GAL4-VP16* V32a P(w+)/CyO was provided by D. St Johnston (University of Cambridge, UK), the salivary gland-specific driver *ftz*-GAL4 lines by C. Doe (University of Oregon, Eugene), the line carrying *His2AvDGFP* by R. Saint (ANU, Canberra, Australia). The lines P[w+=wFRT]101 and ovo^D1, P[w+=wFRT]101; P[ry+=hsFLP38] were obtained from the Bloomington Stock Center.

Generation of germline clones

Germline clones for lethal *east* alleles were produced using the FLP-recombinase dominant female sterility (FLP-DFS) technique (Chou and Perrimon, 1992). Lethal *east*-flippase recombination target (FRT) chromosomes were generated by meiotic recombination of the *east* alleles hop-1, hop-5 and hop-7 with P[w+=wFRT]101 at 14A-B. The presence of the FRT site in lethal recombinants was determined by PCR. The *east*-FRT recombinants were crossed to *ovo*^D1-P[w+=wFRT]101; P[ry+=hsFLP38]. Mitotic recombination in their progeny was induced at the larval third instar stage by heat shock at 37°C for 2 hours. For observations of live embryos, *east*^hop-1-FRT/FM7c was combined with the *His2AvDGFP* marker. Germline clones were induced in *east*^hop-1 FRT/*ovo*^D1; *HistoneGFP*/+ animals. Control germline clones were induced in *y, w,* FRT/*ovo*^D1; *HistoneGFP*/+ larvae.

Expression of GFP-tagged EAST protein

Two versions of EAST (EASTFL: amino acids 1-2336, EASTΔC: aa 1-1573) were expressed with a C-terminally fused green fluorescent protein (GFP) tag using the GAL4 system (Brand and Perrimon, 1993). The corresponding coding regions of the *east* cDNA were joined in frame with the coding region of GFP derived from the vector pEGFP-N1 (Clontech, Palo Alto, CA). The joined fragments were cloned into pUAST (germline transformation vector containing the upstream activating sequence for the GAL4 transcription factor). Transgenic flies were generated using standard P-element-mediated transformation techniques (Spradling, 1986). Expression of EAST–GFP in mitotic cells of embryos was achieved using the ubiquitous drivers *matalpha4-GAL4-VP16*. Expression of EAST–GFP in salivary glands was accomplished using the *ftz*-GAL4 driver.

Immunocytochemistry

Embryos were fixed in 37% formaldehyde as previously described (Tio et al., 1999) and double labeled with mouse anti-EAST (1:1000, ED3) and rat anti-α-tubulin (1:50, Harlan Sera-Lab, Loughborough, UK). Cy3-conjugated goat anti-mouse and Cy5-conjugated donkey anti-rat secondary antibodies were used for detection. Stained embryos were mounted in sonicated phenylenediamine-derived intense fluorochrome (SPIF) (Lundell and Hirsh, 1994) for the detection of DNA and analyzed by laser-scanning confocal microscopy. Testes were dissected out of late male pupae before eclosion. Sex bristles and red eye pigmentation identified mutant *east*^hop-7 males. Dissection and fixation of whole-mount testes was based on a published protocol for squashed testes, which preserves chromosome morphology very well (Bonaccorsi et al., 2000). This protocol also achieved a good preservation of microtubule morphology in prophase and metaphase, but not in prometaphase. In brief, testes were dissected in 0.7% NaCl, fixed in 4% paraformaldehyde in PBS and stained with mouse phospho-histone H3 (Ser10) 6G3 monoclonal antibody (1:200, Cell Signalling Technology, Beverley, MA). Tissues were counterstained with rat anti-α-tubulin and TO-PRO-3 (1:1000, Molecular Probes, Eugene, OR). Images of fluorescently labeled samples were acquired using a Biorad MRC 1024 or a Zeiss LSM 500 laser-scanning confocal microscope.

Live investigation of GFP-tagged proteins

Embryos were collected on yeast-agar plates, dechorionated by hand and transferred to a drop of halocarbon oil (Voltalef S10) on a 32×22 mm coverslip. The coverslip was inverted and, using double-sided tape, attached on top of two columns, which were each composed of two layers of 18×18 mm coverslips, thus allowing oxygen exchange. Embryos in the hanging drop were observed under an upright Zeiss Axioplan microscope attached to a Bio-Rad MRC 1024 confocal laser scanhead. Live images were acquired using a 40× lens and 2× or 3× zoom at 15 second intervals. Third instar larval salivary glands were prepared as previously described (Wasser and Chia, 2000). The cell-permeable nucleic acid dye Syto-17 (Molecular Probes) was used at concentration of 5 μM in Ringer's solution to visualize polytene chromosomes. Image processing was carried out using Confocal Assistant 4.0 and Adobe Photoshop 5.5. Time-lapse movies were assembled using Adobe ImageReady 2.0.

Determination of nondisjunction

Crosses of *east* (*y*+*w*+)/FM7c females against *yw* males were carried out at 25°C. The rates of nondisjunction are based on estimates of the total number of progeny. The numbers of *east/yw* regular daughters (lethal alleles only) were doubled to account for the dead *east*/Y hemizygotes. The numbers of FM7c males were substituted by those of *yw*/FM7c females as FM7c males showed a reduced viability. The numbers of exceptional offspring (*yw* males and *east*/FM7c females) were doubled as their nullo-X (0/0) and triplo-X (*east/yw*/FM7c) siblings are not viable. Hence the rates of nondisjunction (ND) were determined as follows: ND=(2× *yw*+2× *east*/FM7c)/(2× *east/yw*+2× *yw*/FM7c+2× *yw*+2× *east*/FM7c). The segregation defect is specific to achiasmate chromosomes in meiosis I as *east*/+ mothers did not give rise to exceptional progeny. Moreover, the progeny of homozygous *east* germline clones was exclusively female, indicating that they did not produce nullo-X gametes.

Online supplemental information

Quicktime time-lapse videos of post-syncytial embryos expressing GFP-tagged proteins were produced as described in the Materials and Methods section on live investigation of GFP-tagged proteins. The dynamics of EAST–GFP and histone–GFP in mitotic cells were recorded at 15 second intervals. Quicktime Movie 1 corresponds to Fig. 2; Movies 2 and 3 correspond to Fig. 5 (http://jcs.biologists.org/supplemental).

Results

EAST localization in dividing cells

The distribution of EAST protein during the cell cycle was studied in fixed embryos labeled with anti-EAST antibody, anti-tubulin antibody and DNA dye. We analyzed the anti-EAST staining pattern during the synchronous nuclear cycles

of the syncytial blastoderm and during the cell cycles of post-syncytial mitotic domains (Foe, 1989). Consistent with the previously reported ubiquitous expression and nuclear targeting, EAST shows a diffuse nuclear distribution from early interphase (Fig. 1A) until prophase (Fig. 1B). The mitotic distribution from prometaphase onwards can be roughly divided in two stages. In the first stage until metaphase, EAST remains distributed around the condensed chromosomes in the center of the cell. The intensity of anti-EAST immunofluorescence decreases from prometaphase (Fig. 1C) to late metaphase (Fig. 1D), with extrachromosomal signals being stronger than chromosome overlapping signals. The onset of anaphase (Fig. 1E) marks the beginning of the second stage when EAST and chromosomes become spatially decoupled. Sister chromatids are pulled towards opposite spindle poles, whereas the bulk of EAST remains near the position of the previous metaphase plate. Anti-EAST immunofluorescence decreases drastically towards late anaphase (Fig. 1F) and becomes barely detectable at telophase (Fig. 1G). The drastic difference in labeling between telophase and early interphase (Fig. 1H) indicates a rapid accumulation in the daughter nucleus on exit from mitosis. The staining patterns above were observed during the nuclear divisions of the syncytial blastoderm and post-syncytial cell divisions.

EAST–GFP fusion protein in dividing cells of live embryos

To study the temporal and spatial dynamics of EAST localization in dividing cells in vivo, full-length EAST was tagged with a C-terminally fused GFP. Transgenic expression in embryos was achieved using the GAL4-system (Brand and Perrimon, 1993). To test whether this fusion protein (EASTFL–GFP) showed the same localization as the endogenous wild-type (wt) protein, ectopic expression was first performed in salivary glands. EASTFL–GFP, like wt EAST, is targeted to the extrachromosomal and extranucleolar domains of the nucleoplasm (Fig. 2A). As expected, EASTFL–GFP also localizes to the nuclei of diploid embryonic cells. In addition, this GFP-tagged fusion protein appears to show the same functional properties as the untagged counterpart. Ectopic expression of both transgenic proteins in larval salivary gland cells lead to the expansion of END regions between chromosomes and between chromosomes and nuclear lamina. Moreover, persistent overexpression of both proteins in embryos causes lethality (see below).

To analyze the dynamics of EAST localization during mitosis, time-lapse recordings of EASTFL–GFP (Fig. 2C) were compared with those of histone-H2A–GFP (Fig. 2E) (Clarkson and Saint, 1999). Because the ectopic expression of EASTFL–GFP did not discernibly alter the time difference between nuclear envelope breakdown (marked by the diffusion of EASTFL–GFP and histone–GFP from the nucleus into the cytoplasm) (Fig. 2C,E; timepoint +00:00 minutes) and onset of anaphase (stretching of the rounded cell in the case of EASTFL–GFP, +04:45), compared with that of the histone–GFP marker, time-lapse movies of both GFP fusion proteins in different embryos could be aligned. At prometaphase (+01:00), a strongly labeled center surrounded by a dimly labeled peripheral zone indicates that the bulk of EAST–GFP still remains associated with the nuclear remnant. The central fluorescence decays towards late metaphase (+03:00), giving rise to a more evenly distributed fluorescence. At early anaphase (+04:45), EASTFL–GFP clusters along a central line, which corresponds well to the clump of EAST between the segregating sister chromatids seen in fixed tissues (see Fig. 1E). EASTFL–GFP shows a diffuse distribution at late anaphase (+06:15) and telophase. After completion of cytokinesis, EASTFL–GFP is
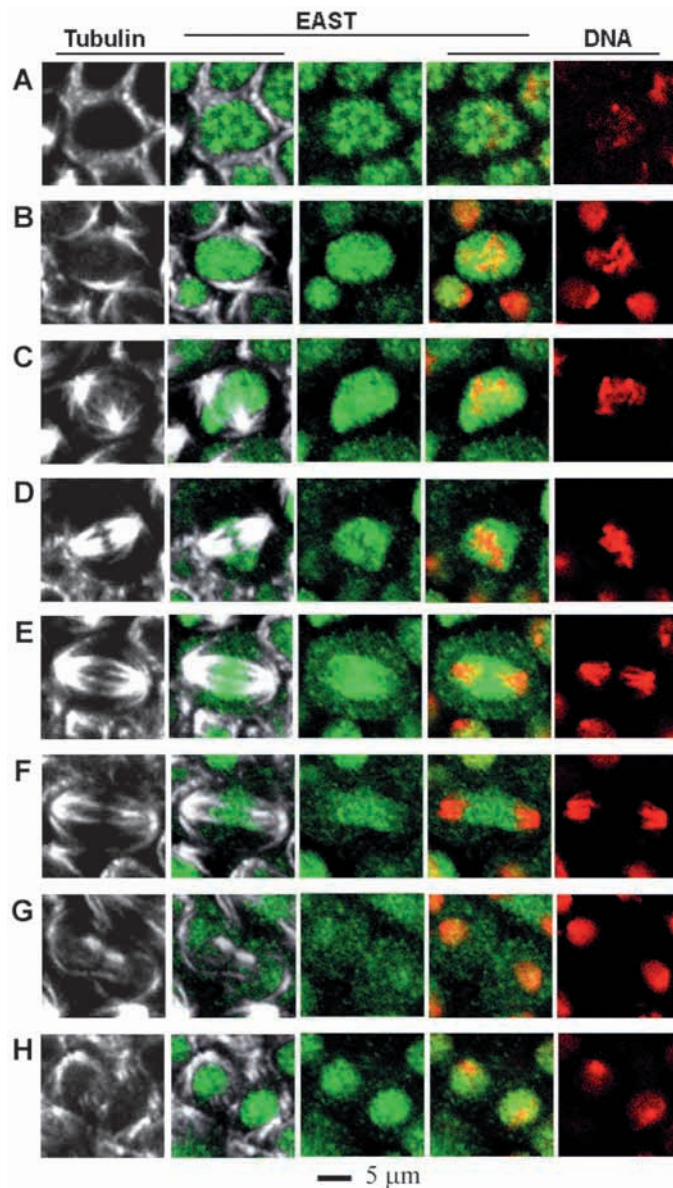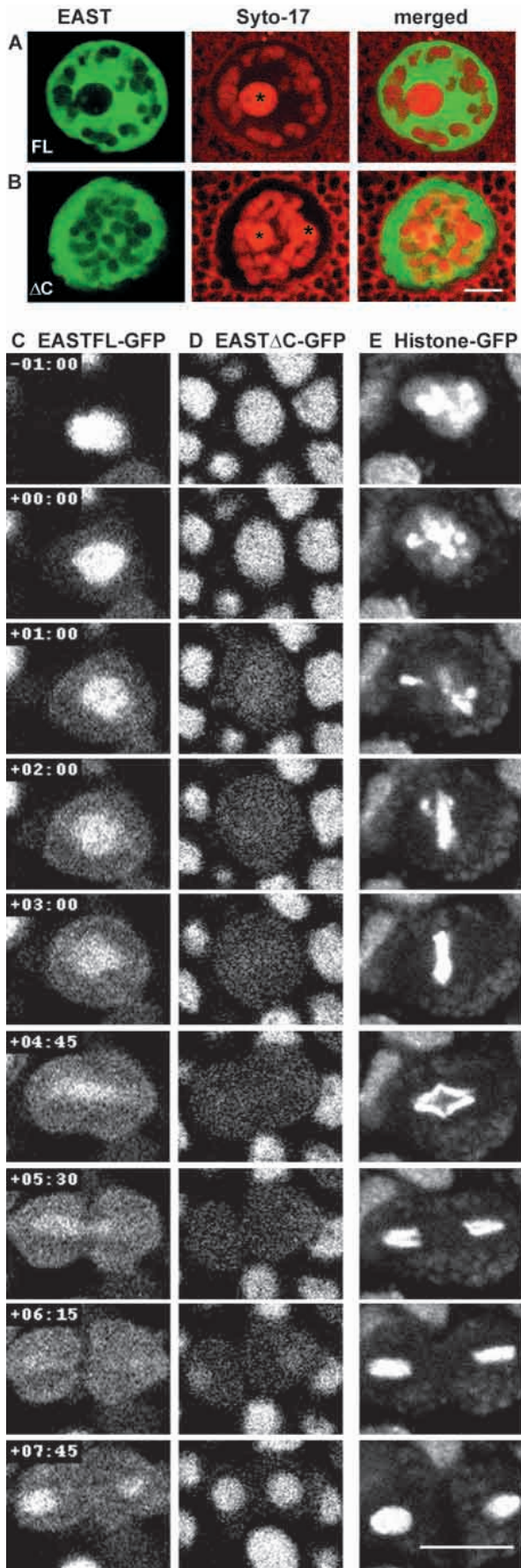

Fig. 1. Localization of EAST protein in dividing cells. The distribution of EAST in cells of mitotic domains was revealed by triple labeling post-syncytial embryos with anti-EAST antibody (green), anti-tubulin antibody (white) and DNA dye (red). Throughout interphase (A,H) and prophase (B), EAST shows nuclear localization. At prometaphase (C), metaphase (D) and early anaphase (E), EAST remains in the center of the cell associated with the remnant of the interphase nucleus. EAST labeling decays at late anaphase (F) and is barely detectable at telophase (G). Intense staining is again seen in early interphase (H).

Fig. 2. EAST–GFP fusion proteins during mitosis of live embryos. Two versions of EAST, EASTFL(1-2336)–GFP (A,C) and EASTΔC(1-1573)–GFP (B,D), were ectopically expressed using the GAL4 system and studied in vivo using confocal microscopy (also see Movie 1, http://jcs.biologists.org/supplemental). (A,B) In larval salivary glands, the two EAST–GFP species (green) preferentially localize to extrachromosomal and extranucleolar regions of the nucleus. Chromosomes were labeled with the in vivo nucleic acid marker Syto-17 (red), which also labels ribosomal RNA in the nucleolus (*) and cytoplasmic RNA. (C,D) In dividing embryonic cells during germband extension, images of EAST–GFP fusion proteins were acquired at 15 second intervals. (E) The live recording of a third embryo expressing histone-H2A–GFP is displayed for comparison. The onset of prometaphase, when GFP-tagged proteins begin to leak into the cytoplasm, presumably due to nuclear envelope breakdown, was chosen as timepoint zero (+00:00). Both full-length and truncated versions of EAST show nuclear localization in interphase (–01:00). However, they differ in their behavior during mitosis. EASTFL (C) remains enriched in the central part of the cell until anaphase (+04:45), whereas its truncated counterpart EASTΔC (D) rapidly disperses at prometaphase (+01:00) and shows diffuse distribution until telophase (+06:15). After cytokinesis (arrows indicate cleavage furrow), both forms of EAST–GFP are recruited back to the daughter nuclei (+07:45). Bars, 10 μm; bar in B also applies to A; bar in E also applies to C and D.

rapidly recruited to the daughter nuclei (+7:45). In summary, the distribution of EAST revealed by real-time analysis is in good agreement with its distribution derived from fixed tissues. EAST remains associated with the remnant of the interphase nucleus until early anaphase and becomes incorporated into the newly assembled interphase on exit from mitosis.

The C-terminus of EAST is required for association with the mitotic remnant of the nucleus

A truncated version of EAST comprising the first 1573 residues coupled to GFP (EASTΔC–GFP) was also analyzed in vivo. This fusion protein, like its full-length counterpart, which contains the N-terminal 2332 residues, is imported into interphase nuclei of all developmental stages and preferentially accumulates in extrachromosomal regions of giant larval nuclei (Fig. 2B), showing that the N-terminal two thirds of EAST are sufficient for nuclear import and correct intranuclear distribution. However, the C-terminally deleted fusion protein differs from the full-length version in its behavior during mitosis (Fig. 2D). During prometaphase (+01:00), EASTΔC–GFP quickly disperses into the cytoplasm and does not associate with a central nuclear remnant. Its distribution remains diffuse until it accumulates again in the daughter nuclei at early interphase (+07:45). The failure of this fusion protein to be retained in the center of the cell at prometaphase suggests that the C-terminus of EAST is required for its anchorage to the remainder of the nucleus that has been stripped of its outer shell (nuclear envelope and lamina). Moreover, EAST–GFP and EASTΔC–GFP show differences in toxicity, if expressed from the ubiquitous *daughterless*–GAL4 driver. Persistent overexpression of EASTFL–GFP or wt EAST causes embryonic lethality, whereas EASTΔC–GFP overexpression does not affect development to viable adulthood.
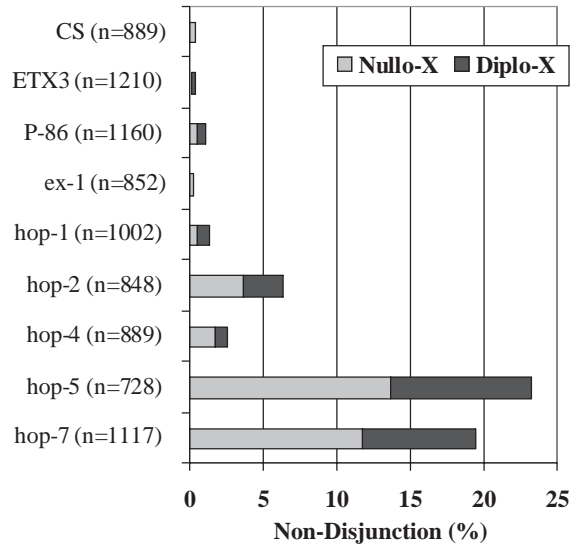
Fig. 3. Mutations in *east* cause nondisjunction (ND) of achiasmate X-chromosomes in female meiosis. Females carrying different X-chromosomes over the FM7c balancer were crossed with *yw* males. The bar chart compares the rates of ND of X-chromosomes from wt (CS), the viable *east* insertion allele ETX3, the viable revertant P86 and six lethal reversion alleles (Wasser and Chia, 2000). To determine frequencies of ND, the numbers of nullo-X (*yw* males) and diplo-X (*w*+/FM7c) exceptional offspring were scored. The original insertion line ETX3 shows normal segregation, whereas some of the lethal alleles show ND rates of up to 20%. Note that the partial deletion *east*hop-7 is associated with more than 20× higher frequency of ND than the complete deletion *east*hop-1 of the *east* transcription unit. n, total number of flies scored.

Mutations of *east* affect chromosome segregation during female meiosis

Mutations of *east* dominantly interfere with the segregation of achiasmate chromosomes in female meiosis. Females carrying *east* mutations over the X-chromosome balancer FM7c produced exceptional gametes, which contained either none or two X-chromosomes (Fig. 3). Defects in meiosis were only associated with lethal *east* alleles. Five out of ten recessive lethal alleles displayed nondisjunction (ND) frequencies ranging from 2.6% to 23.7%, whereas all four viable *east* alleles tested were not affected. The wt X-chromosome over FM7c displayed a ND rate of 0.4%. A ND rate of up to 1% has been reported for control X-chromosomes over the FM7c balancer (Moore et al., 1994). Because the original P-element insertion ETX3 (the parental strain from which the various *east* alleles were derived) balanced over FM7c was not associated with a significant ND rate, this phenotype probably resulted from imprecise excisions of the P-element out of the *east* locus. The segregation of *east* X-chromosomes from wt X-chromosomes was not perturbed, suggesting the phenotype is specific to achiasmate chromosomes. Even homozygous *east* germline clones did not give rise to exceptional progeny (see below). Genetic tests also showed that ND occurs during the segregation of homologs in meiosis I and not during the segregation of sister chromatids in meiosis II (see Materials and Methods). The highest frequencies of ND were

Table 1. Removal of maternal *east* expression

east allele	Heterozygous *east*/FM7c maternal germline (%)	Homozygous *east* maternal germline (%)
hop-1	58 (*n*=216)	80 (*n*=230)
hop-5	12 (*n*=178)	95 (*n*=250)
hop-7	8 (*n*=177)	32 (*n*=250)

The loss of maternal *east* increases embryonic lethality compared with the loss of zygotic expression alone. Females with germline cells that were either heterozygous or homozygous for three different *east* alleles were mated with FM7c males. Dead embryos were scored 24 hours after egg collection. (The percentages of dead *east*/FM7c and *east*/Y embryos derived from heterozygous mothers might be overestimated because all embryos carrying only balancer X-chromosomes were assumed to be viable.)

associated with the 5′ deletion of the *east* transcription unit (*east*hop-7) and a deletion of the upstream region (*east*hop-5) (Wasser and Chia, 2000). ND was limited to achiasmate X-chromosomes. Similar to previously identified mutants, *east* does not affect the segregation of the achiasmate chromosome 4 (Sekelsky et al., 1999). Apart from the ND phenotype, heterozygous *east* females did not show any other discernible abnormalities.

Loss of *east* function increases the frequency of mitotic defects

The presence of *east* mRNA in unfertilized eggs (VijayRaghavan et al., 1992) and the detection of EAST protein in nuclei of the syncytial blastoderm stage indicate maternal expression. To study a possible role of *east* in the mitosis of early embryos, the maternal component of *east* expression *east(mat)* was removed by generating germline clones for the three lethal alleles *east*hop-1, *east*hop-5 and *east*hop-7 using the DFS-FRT technique (Chou and Perrimon, 1992). Maternal *east* expression is not essential for viability because, for all three alleles tested, some of the embryos lacking the maternal component and carrying only one paternal wt copy of the *east* gene can still develop into fertile females. However, the presence of maternally provided *east* gene products improves the rate of survival (Table 1). Although some heterozygous embryos without maternal *east* developed into normal adults (Fig. 4A,B), others showed severe developmental defects that resulted in embryonic lethality (Fig. 4C,D). The X-chromosomal FM7-Act-GFP balancer was used to determine the lethality of *east*hop-1 (maternal –/–, zygotic +/–) embryos; the lack of maternal *east* was lethal for approximately 40% of zygotically heterozygous *east* embryos. Such heterozygous adults often (around 25% of escapers for allele *east*hop-1) lacked body structures such as tergites on the abdominal cuticle or one of the legs (Fig. 4B). This phenotype was never observed in females born as control germline clones (maternal +/+, zygotic +/–) or in heterozygous *east* flies (maternal +/–, zygotic +/–) that inherited maternal gene products from heterozygous mothers.

To examine the consequences of loss of *east* on the synchronous nuclear cycles of the syncytial blastoderm, embryos lacking germline *east* were stained with anti-histone and antitubulin antibodies. In a small proportion of syncytial embryos (approximately 10% in *east*hop-1 or *east*hop-5), vast areas of the embryonic surface were depleted of nuclei (Fig.
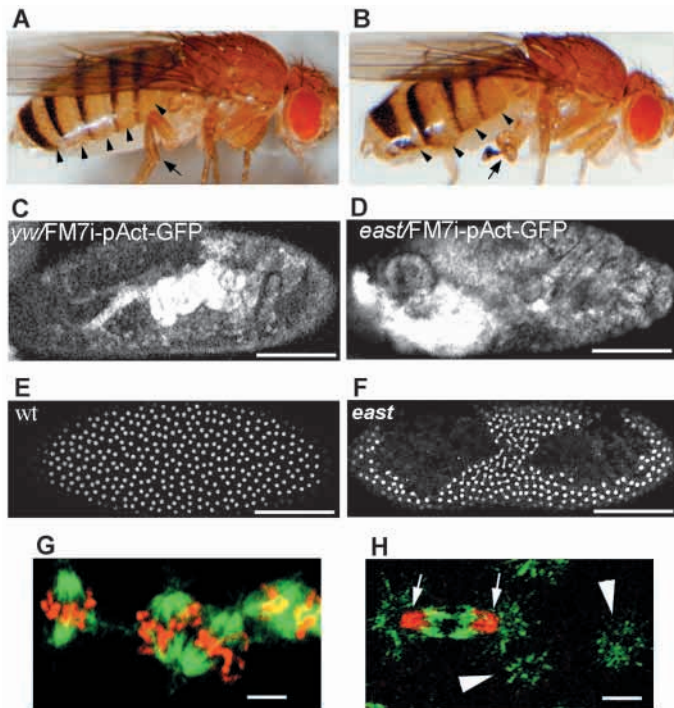
Fig. 4. Loss of maternal *east* results in pleiotropic mitotic and developmental defects. Loss of maternal *east* expression in *east*[hop-1] germline clones coupled with zygotic expression from one wt copy of *east* can lead to a variety of phenotypes, ranging from fertile female escapers without discernible morphological abnormalities (A), to adults showing a loss of various morphological structures (B), like tergites on the abdomen (arrowheads) or appendages (arrow). Lethality, along with variable developmental defects, was also observed during embryonic development. In late control embryos (C), the in vivo GFP marker of the balancer FM7i-pAct–GFP labels the midgut. (D) Loss of maternal *east* can cause the GFP expression to appear in the anterior regions of the embryo. (E,F) Nuclei of the syncytial blastoderm stage in wt (E) and *east(mat)* (F) embryos stained with anti-histone antibody. Loss of maternal *east* can lead to the elimination of nuclei from the surface (F). (G,H) Syncytial blastoderm embryos stained with anti-tubulin (green) and anti-histone (red) antibodies. (G) Polyploid nuclei at metaphase and (H) orphan centrosomes in anaphase (arrowheads) without daughter nuclei (arrows) indicate mitotic errors. Bars, 100 μm (C-F) and 10 μm (G-J).

Table 2. Nuclear cycles in control and *east*[hop-1] germline clones

NC	Genotype	#E	#N	Mitotic defects (%)	Nuclear density (nuclei/10,000 μm^2)
11	Control	3	79	1.3	41
	east	4	74	6.8	40
12	Control	9	390	1.5	70
	east	13	457	6.1	68
13	Control	9	551	0.7	139
	east	12	790	2.5	122
14	Control	8	1116	0	289
	east	9	1030	0	233

Live recordings of control and *east*[hop-1] germline clones expressing the histone–GFP chromosome marker during the nuclear cycles (NC) of the syncytial blastoderm stage. The average frequencies of mitotic defects, nuclear densities and durations from onset of anaphase of the previous cycle to end of the metaphase of the indicated cycle are shown. #E, number of embryos; #N, number of nuclei scored.

east[hop-1] FRT were compared to *yw* FRT control germline clones. Live recordings starting from either nuclear cycle 11 or 12 and ending in early interphase of cycle 14 were acquired for 14 mutant *east* and 11 control embryos. The subset of nuclei observed represented approximately 4% of the nuclei on the surface of each embryo (see Materials and Methods). To quantify mitotic errors, the numbers of nuclei that showed delayed condensation in prophase, failed to separate completely in anaphase, remained condensed in the following interphase and subsequently dropped into the interior of the egg were scored (Table 2). The error frequencies were up to four times higher in mutant than wild-type embryos. The absolute average numbers of nuclei affected were less than 7%. More faulty divisions were observed in the faster nuclear cycle (NC) 12 than in the slower NC 13. The density of nuclei was slightly reduced in mutants compared to wt in NC 13 and 14. Only in one case (out of 14) did we see a large patch of nuclei in a mutant embryo sinking into the interior after an apparently normal NC 12. The resulting hole was found to cover around one third of the surface. In summary, the studies on syncytial blastoderm embryos did not provide any evidence that *east* plays an essential or crucial role in the progression of nuclear cycles. However, the increase in the frequency of mitotic abnormalities that are observed when maternal *east* is removed indicates that it plays an important role in promoting the efficiency and accuracy of the process.

Removal of *east* affects the congression of chromosomes at prometaphase

Live observations of *east*[hop-1] (maternal –/–) embryos carrying the histone–GFP marker were also extended to mitotic domains, clusters of synchronously dividing cells of post-syncytial embryos (Foe, 1989). A subset of dividing cells in mutant embryos displayed abnormal chromosome movements during prometaphase. During prometaphase of wt cells, chromosomes usually remain clustered in the center of the cell and become aligned in a plate-like configuration that is oriented perpendicular to the future axis of division (Fig. 5A, +2:00 minutes). In mutant cells, two types of unusual maneuvers were observed. On nuclear envelope breakdown,

4F). This phenotype was not observed in control embryos (Fig. 4E). We observed a variety of mitotic abnormalities in a small subset of nuclei, including incomplete separation of chromosomes at anaphase, resulting in polyploid nuclei (Fig. 4G) and nuclei dropping from the surface into the interior of the egg, leaving behind orphan centrosomes at the cortex (Fig. 4H). Interestingly, other maternal-effect mutations were also reported to cause both an elimination of nuclei in embryos of the syncytial blastoderm stage and missing appendages in surviving adults (Sullivan et al., 1990; Zalokar et al., 1975).

Nuclear cycles in live embryos lacking maternal east

To test whether loss of maternal *east* caused any subtle phenotypes that might not be discernible in fixed embryos, we studied the synchronous nuclear cycles in vivo using the histone–GFP marker. Germline clones of the genotype
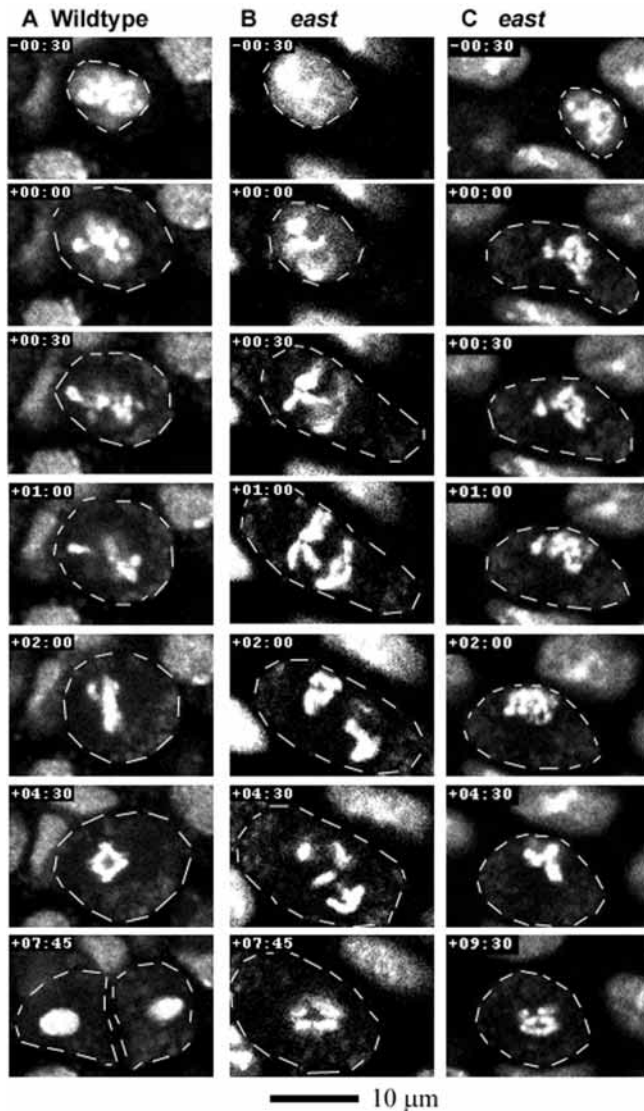
Fig. 5. Loss of *east* leads to abnormal movements of chromosomes during prometaphase. Time-lapse recordings of cell divisions in mitotic domains of live embryos expressing histone–GFP reveal irregular patterns of congression to the metaphase plate (see Movies 2 and 3, http://jcs.biologists.org/supplemental). The beginning of prometaphase is chosen as timepoint zero. (A) In control embryos, on nuclear envelope breakdown, condensed chromosomes remain clustered in the center of the cell and rapidly orient themselves perpendicular to the future axis of division (+02:00). (B) In *east(mat)*hop-1, chromosomes were seen to break up into distinct clumps of DNA or (C) to stray to the periphery of the cell. Compare A and C at timepoint +02:00 minutes: chromosomes in the wt cell are aligned centrally perpendicular to the future axis of division, whereas the chromosomes in *east* mutant cell are positioned near the cell cortex parallel to the future axis of division. Compare the three live recordings at timepoint +04:30 minutes: while chromosomes in the control cell are undergoing anaphase (A), chromosomes in the *east* cells are still split up into distinct groups (B) or located near the cortex in an abnormal orientation (C). However, with a time delay, chromosomes in mutant cells eventually manage to arrive in the center and complete mitosis. Stippled lines outline the boundaries of the cells.

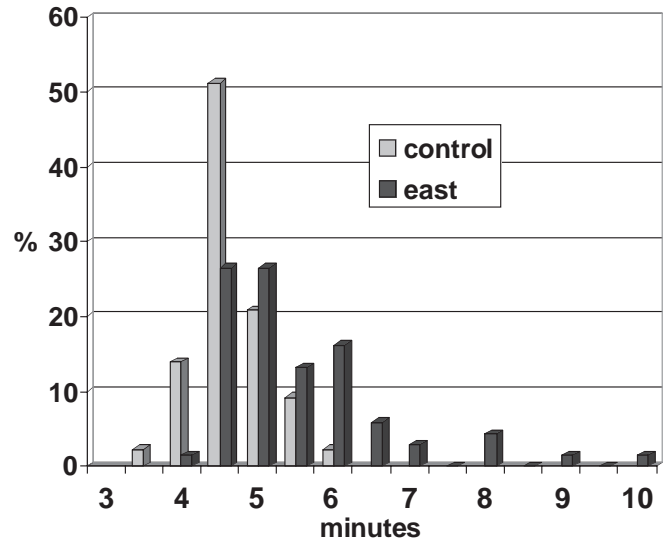chromosomes moved away from each another, giving rise to spatially separated groups of chromosomes instead of one

Fig. 6. Duration (minutes) of prometaphase and metaphase in mitotic domains of *east*hop-1 (*n*=68 divisions) and control (*n*=43 divisions) germline clones. Note that the maxima in distribution of controls and mutants are close together. However, although control cells show a symmetric distribution, mutant cells display a more skewed pattern, reflecting a greater variability in the duration of chromosome congression.

contiguous cluster (Fig. 5B, +1:00 to +4:30). Distinct clusters of chromosomes in prometaphase were observed in 44% of mutant cells (30 out of 68 in 15 embryos). By comparison, 14% of control cells (6 out of 43 in 8 embryos) showed a disjoint configuration at this stage that never appeared as dramatic as in mutants. At a lower frequency (5-10%), chromosomes in *east* cells strayed away from the center of the cell towards the plasma membrane (Fig. 5C). This phenotype was never seen in control embryos. Abnormal movements of chromosomes during congression to the metaphase plate were associated with a delayed onset of anaphase. In controls, the onset of anaphase occurred 3.5-6.0 minutes (average 4.5±0.5) after the beginning of prometaphase (see Fig. 6 for distribution diagram). The same period in *east* (maternal –/–) embryos showed a higher degree of variability, ranging from 4.0 to 9.75 minutes (average 5.4±1.1). Discrepancies in duration and choreography of chromosome congression could be seen within the same mitotic domain; e.g. seven cells of one *east* mutant mitotic domain entered mitosis and spent the following different times in prometaphase and metaphase: 5.75, 4.75, 8.0, 9.0, 4.75, 4.5, 9.75 minutes (cells entered mitosis in the same order as their respective time periods are listed). Apart from one case, all cells eventually entered anaphase and completed mitosis. In summary, these observations suggest that *east* might contribute to the process of chromosome alignment by constraining the mobility of chromosomes at prometaphase. Loss of *east* can therefore lead to a delay of chromosome congression, but not to mitotic arrest.

Abnormal chromosome behavior in spermatocytes

To test whether the loss of *east* might affect meiosis, the testes of *east*hop-7 hemizygotes in the late pupal stage were stained with an antibody against histone H3 phosphorylated at
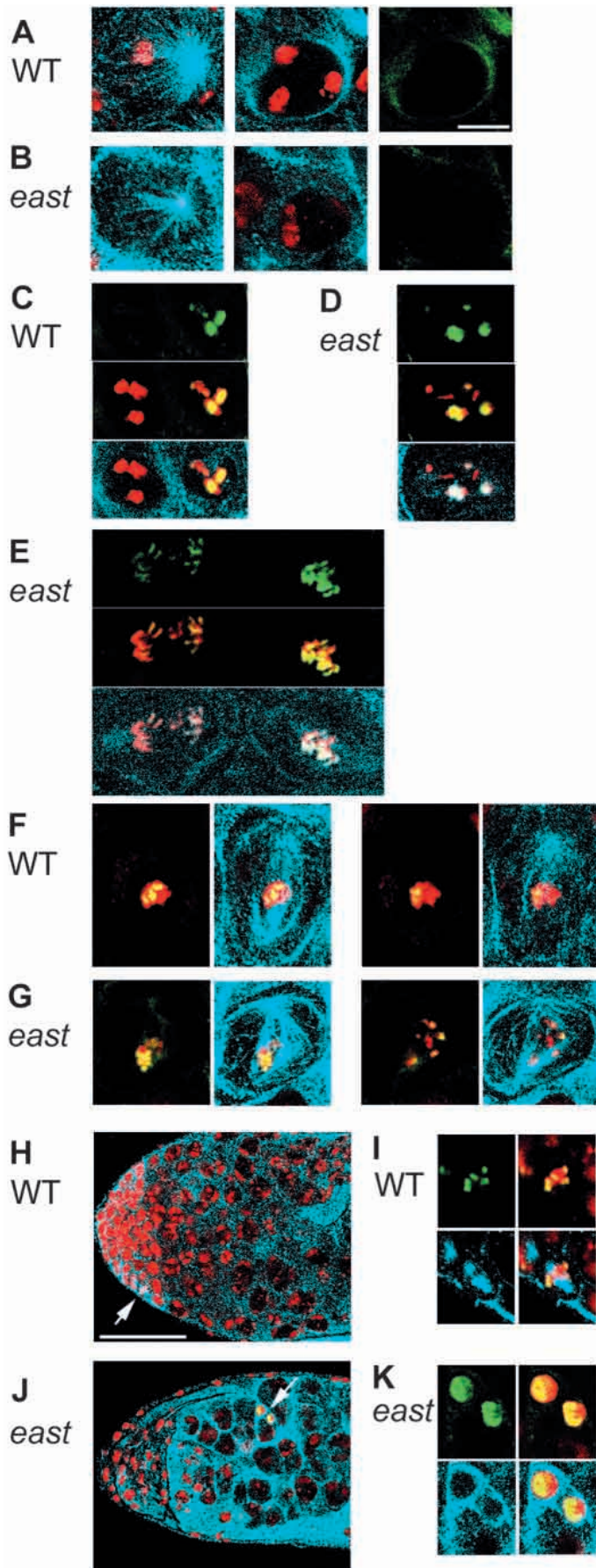
serine10 (PH3). PH3 labeling is correlated with chromosome condensation and allows the identification of dividing cells between prophase and anaphase (Hendzel et al., 1997; Wei et al., 1998). We observed abnormalities in different stages of meiosis I. In early prophase of wt primary spermatocytes, characterized by aster formation and lack of PH3 labeling, the replicated genome is organized into three or four spatially separated clusters of DNA (Fig. 7A) (Cenci et al., 1994). In *east* mutants, DNA appears to be more diffuse and does not aggregate into distinct clumps (Fig. 7B). A lower intensity of TO-PRO-3 staining indicates a lower degree of DNA condensation. The clustering of chromosomes in wt is preserved through the onset of H3 phosphorylation later in prophase until prometaphase when the nuclear envelope breaks down (Fig. 7C). During the beginning of H3 phosphorylation in *east* spermatocytes, chromosome clusters continue to show differences in shape and quantity from wt controls. The quantity of clumps of DNA can exceed four (Fig. 7D) and chromosomes can show a more scattered distribution (Fig. 7E). In contrast to the tightly packed organization of condensed chromosomes in wt cells, loose chromosome arms can be

Fig. 7. Abnormal behaviour of chromosomes in *east* spermatocytes. Wild-type and *east*[hop-7] testes were labeled with antibodies to PH3 (green) and α-tubulin (cyan). DNA was detected with TO-PRO-3 (red). (A,B) Primary spermatocytes in early prophase. The stage is inferred from the nucleation of astral microtubules (left panels). The central panels show the nuclei of the same cells in focal planes 3 μm below. Chromosomal DNA in wt is highly condensed and organized into three distinct clusters. DNA in the *east* spermatocytes is less condensed and does not show discernible clustering. Chromosomal DNA does not show any H3 phosphorylation (right panels, same focal planes as middle panels). The green label is due to a cross-reaction of the antimouse secondary with the rat primary antitubulin antibody. In C-E: top panels, PH3 labeling (green); middle panels, PH3+DNA labelings; bottom panels, PH3+DNA+α-tubulin labelings. (C) As wt cells progress towards late prophase (left cell) and prometaphase (right cell), PH3 labeling can be detected, apparently coinciding with nuclear envelope breakdown (right cell). The organization of chromosomes into three clumps of DNA is maintained. (D) In *east* prometaphase, the number of DNA clumps can exceed four; here, two major and four minor clusters can be observed. (E) Two neighbouring spermatocytes of the same cyst in an *east* testis display different intensities of PH3 labeling (weak in the left, strong in right cell), suggesting that these cells are at the beginning of prometaphase. The chromosomes appear scattered and their arms become exposed and visible. By contrast, chromosome arms are not discernible in wt primary spermatocytes (C). (F,G) Primary spermatocytes during metaphase of wt (F) and *east* (G) testes. Left and right panels show focal planes of the same cells 2 μm apart. (F) In wt, chromosomes congregate to a single cluster in the middle of the spindle. (G) In *east*, some of the chromosomes (right panel) disperse away from the main DNA cluster (left panel). (H,J) Testes of wt (H) and *east* (J) pupae containing PH3-positive cells (arrows) that are shown in higher magnifications in (I) for wt and (K) for *east*. In (I,K): top left panels, PH3; top right, PH3+DNA; bottom left, tubulin; bottom right, PH3+DNA+tubulin. (J,K) Testes in *east* pupae contain small cells with PH3-positive nuclei (arrow), presumably spermatogonia. (I,H) In wt, small PH3-positive cells located near the tip of the testis are stem cells and spermatogonia that undergo mitosis. Note that the abnormal PH3-positive cells in *east* are not associated with mitotic spindles as in wt (I,K; compare bottom panels). Bar in (A) represents 10 μm and applies to all panels except (H,J). Bar in (H) equals 50 μm and also applies to (J).

observed in mutants. During metaphase in wt cells, the bivalents are captured by the spindle and congregate to form one cluster (Fig. 7F). Approximately 50% of *east* primary spermatocytes in metaphase exhibited an abnormal arrangement of chromosomes. Chromosomes were observed to stray away from the major cluster and adopt a more scattered configuration (Fig. 7G).

Furthermore, mutant (Fig. 7J,K), but never wt (Fig. 7H,I) testes, contained cells with round and condensed PH3-positive chromosomes. These cells, which were observed throughout the testes individually or in groups of two, showed cortical tubulin staining that is characteristic of interphase cells (Fig. 7K, bottom panels), although PH3 only marks mitotic cells in wt. Because the size of these cells was much smaller than that of primary spermatocytes, we infer that they are probably spermatogonia arrested in mitosis. By contrast, PH3-positive cells of similar size in wt were located near the tip of the testis and showed chromosome and microtubule morphologies characteristic of mitotic cells (Fig. 7H,I).

Discussion

The original observation that EAST overexpression can dramatically change the nuclear architecture of postmitotic polyploid cells (Wasser and Chia, 2000) prompted us to explore the possibility that loss of *east* function might alter the chromosome organization of dividing cells. The cell-cycle-dependent localization of EAST resembles those of other nuclear proteins such as CP60 or Tpr (Oegema et al., 1997; Zimowska et al., 1997), which occupy extrachromosomal territories of the nuclear interior during interphase and, even after NE breakdown, continue to associate with structures of the nucleus that persist into mitosis. This common localization of several different proteins supports the idea of a nuclear endoskeleton that is preserved from interphase to metaphase, dismantled at anaphase before cytokinesis and reassembled after exit from mitosis. Live observations indicate that, during mitosis, EAST is gradually released from this nuclear remnant into the cytoplasm and later recycled for the reassembly of the interphase nucleus. The temporal and spatial pattern of the internal nuclear structure is distinct from that of the nuclear shell (NE, lamina and associated proteins) that disassembles earlier at prometaphase.

Possible role of a nuclear remnant in mitosis

Not even a complete deletion of the *east* locus causes a block or any other catastrophic defect in cell-cycle progression, therefore we can rule out whether *east* has any obligatory function in cell division. However, the loss-of-function phenotypes suggest that its activity contributes to the accuracy and efficiency of mitosis and meiosis. EAST, as a component of an internal nucleoskeleton, appears to facilitate the congression of chromosomes at prometaphase by constraining their mobility (Fig. 8). During prometaphase in embryonic *east* mutant cells, chromosomes were observed to adopt a more relaxed configuration than in wt, drift apart from one another and tumble from central to cortical regions of the cell. The abnormal movements can delay the onset of anaphase. These observations suggest that, although the disassembly of the nuclear exoskeleton (NE, lamina) has to take place to
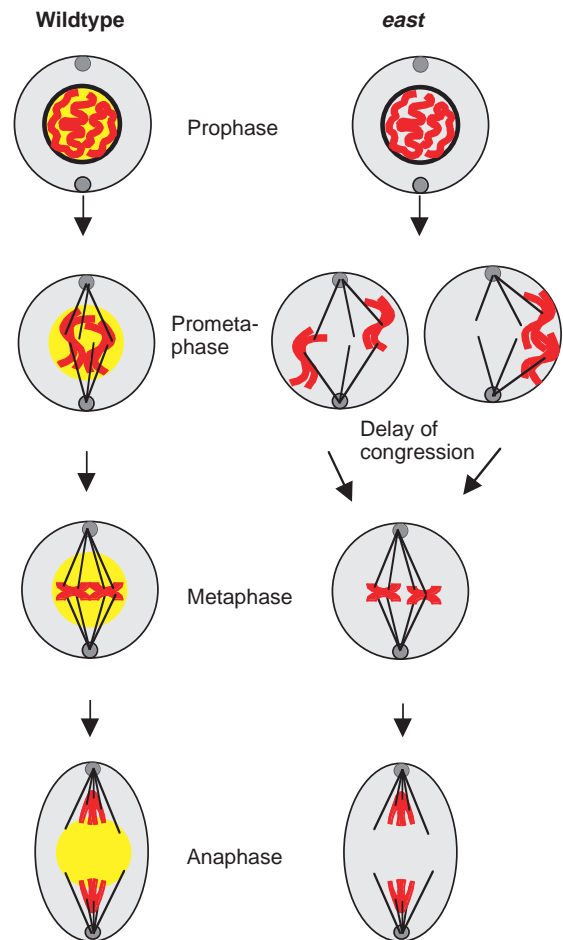

Fig. 8. Model proposing how EAST, as part of an internal nucleoskeleton, could facilitate the congression of chromosomes at prometaphase. Even after nuclear envelope breakdown, chromosomes remain embedded in a nucleoskeleton that constrains their mobility and helps them to remain clustered in the center of the cell. Loss of *east* might disrupt this structure, causing condensed chromosomes to stray away from the center of the cell or from one another.

allow interactions between chromosomes and microtubule spindle, an intact nuclear endoskeleton seems to be required to keep chromosomes clustered together in the central region of the cell. The abnormal movements of chromosomes, resulting in a delay of anaphase, were limited to cell divisions and not detected during the syncytial nuclear cycles. An explanation might be that mitosis in syncytial embryos is semiclosed, which means that the lamina is only punctured and not dissolved until late in metaphase when chromosome alignment is completed (Paddy et al., 1996). Therefore, during the nuclear cycles, the lamina limits the mobility of chromosomes.

Functional studies on other proteins of a putative nucleoskeleton are rare. Antibody perturbation studies of the nuclear Skeletor protein showed a role in spindle assembly during mitosis (Walker et al., 2000). Similarly, the abnormal chromosome movements in *east* embryos during metaphase might result from the disruption of a spindle matrix that is composed of nuclear proteins and guides the outgrowth of the

spindle. However, two lines of evidence argue against this possibility. First, EAST, unlike Skeletor, does not show colocalization with the mitotic spindle at metaphase. Second, abnormal DNA staining patterns can be detected in prophase of male meiosis before the NE breaks down and chromosomes establish interactions with spindle microtubules.

In contrast to higher mobility resulting from a loss of function, the gain of function of *east* can impose additional constraints on the mobility of chromosomes. Within the spatial limits of the nuclear envelope, the expansion of the END caused by the overexpression of EAST can lead to an exclusion of chromosomes from a ring zone underneath the lamina in larval salivary cells (see Fig. 2A,B) and spermatogonia (Wasser and Chia, 2000). A study on chromosome motion in live *Drosophila* spermatocytes showed evidence of constraints on the mobility of chromosomes inside the interphase nucleus (Vazquez et al., 2001). The constraints in mobility were proposed to be mediated by the interactions of chromosomes with the nuclear envelope and other internal nuclear structures.

Interphase chromosome organization and chromosome inheritance

A nucleoskeleton could also assist in the segregation of nonexchange chromosomes in meiosis. Chiasmata formation assures the alignment of homologous chromosomes and their co-orientation during metaphase of meiosis I. Genetic studies in *Drosophila* have established that a backup system termed 'distributive disjunction' helps to partition even those chromosomes (such as balancers) that do not undergo homologous recombination. Achiasmate chromosomes are paired via heterochromatic regions throughout prophase of meiosis I, disjoin at metaphase and are positioned towards opposite spindle poles, whereas chiasmate chromosomes remain in a central chromatin mass (Dernburg et al., 1996; Karpen et al., 1996; Theurkauf and Hawley, 1992). A reasonable explanation for the high frequency of nondisjunction observed for multiple *east* alleles is that, following nuclear envelope breakdown in *east* mutant oocytes, paired achiasmate homologues might, due to a defective nucleoskeleton, drift away from the zone previously occupied by the nucleus. In this scenario, two homologues, after splitting up, could end up near the same spindle pole and, at anaphase, be partitioned to the same daughter nucleus. A link between chromosome organization and chromosome transmission has been shown for genes involved in position effect variegation (PEV). Su(var)2-10 regulates chromosome structure and organization and is required for the faithful inheritance of chromosomes (Hari et al., 2001).

Our data on primary spermatocytes are consistent with an involvement of *east* in the spatial arrangement of chromosomes. During prophase and prometaphase of male meiosis I, chromosomes are normally clustered into three major spatially separated clumps of DNA (Cenci et al., 1994). In *east* mutant spermatocytes, both the shape and number of DNA clusters differ from wt, indicating a defective spatial organization of chromosomes within the nucleus. A recent study on live cultures of spermatocytes showed that homologous chromosomes and sister chromatids separate in late G2 (Vazquez et al., 2002). It was proposed that, besides heterochromatic association and chromatin entanglement,

pairing of homologous chromosomes is maintained by restricting the homologs to discrete chromosome territories. Our data are consistent with the notion that the EAST protein might be involved in stabilizing these chromosome territories.

In summary, our data support the model that chromosomes in the interphase nucleus and in mitosis are embedded into a structure that can restrict their mobility. The putative nuclear endoskeleton has to be elastic and permeable, thus permitting movements of chromosomes and penetration of the microtubule spindle. The challenge ahead lies in identifying additional components of this nuclear structure, and further understanding of how EAST, as well as these components, act.

References

Bonaccorsi, S., Giansanti, M. G., Cenci, G. and Gatti, M. (2000). Cytological analysis of spermatocyte growth and male meiosis in *Drosophila melanogaster*. In *Drosophila Protocols* (ed. W. Sullivan, M. Ashburner and R. S. Hawley), pp. 87-117. Cold Spring Harbor, New York: Cold Spring Harbor Laboratory Press.

Brand, A. H. and Perrimon, N. (1993). Targeted gene expression as a means of altering cell fates and generating dominant phenotypes. *Development* **118**, 401-415.

Cenci, G., Bonaccorsi, S., Pisano, C., Verni, F. and Gatti, M. (1994). Chromatin and microtubule organization during premeiotic, meiotic and early postmeiotic stages of *Drosophila melanogaster* spermatogenesis. *J. Cell Sci.* **107**, 3521-3534.

Chou, T. B. and Perrimon, N. (1992). Use of a yeast site-specific recombinase to produce female germline chimeras in Drosophila. *Genetics* **131**, 643-653.

Clarkson, M. and Saint, R. (1999). A His2AvDGFP fusion gene complements a lethal His2AvD mutant allele and provides an in vivo marker for Drosophila chromosome behavior. *DNA Cell Biol.* **18**, 457-462.

Dernburg, A. F., Sedat, J. W. and Hawley, R. S. (1996). Direct evidence of a role for heterochromatin in meiotic chromosome segregation. *Cell* **86**, 135-146.

Foe, V. E. (1989). Mitotic domains reveal early commitment of cells in Drosophila embryos. *Development* **107**, 1-22.

Giansanti, M. G., Bonaccorsi, S. and Gatti, M. (1999). The role of anillin in meiotic cytokinesis of Drosophila males. *J. Cell Sci.* **112**, 2323-2334.

Hari, K. L., Cook, K. R. and Karpen, G. H. (2001). The Drosophila Su(var)2-10 locus regulates chromosome structure and function and encodes a member of the PIAS protein family. *Genes Dev.* **15**, 1334-1348.

Hendzel, M. J., Wei, Y., Mancini, M. A., Van Hooser, A., Ranalli, T., Brinkley, B. R., Bazett-Jones, D. P. and Allis, C. D. (1997). Mitosis-specific phosphorylation of histone H3 initiates primarily within pericentromeric heterochromatin during G2 and spreads in an ordered fashion coincident with mitotic chromosome condensation. *Chromosoma* **106**, 348-360.

Karpen, G. H., Le, M. H. and Le, H. (1996). Centric heterochromatin and the efficiency of achiasmate disjunction in Drosophila female meiosis. *Science* **273**, 118-122.

Lundell, M. J. and Hirsh, J. (1994). A new visible light DNA fluorochrome for confocal microscopy. *Biotechniques* **16**, 434-440.

Matakatsu, H., Tadokoro, R., Gamo, S. and Hayashi, S. (1999). Repression of the wing vein development in Drosophila by the nuclear matrix protein plexus. *Development* **126**, 5207-5216.

Moir, R. D., Spann, T. P., Lopez-Soler, R. I., Yoon, M., Goldman, A. E., Khuon, S. and Goldman, R. D. (2000). Review: the dynamics of the nuclear lamins during the cell cycle– relationship between structure and function. *J. Struct. Biol.* **129**, 324-334.

Moore, D. P., Miyazaki, W. Y., Tomkiel, J. E. and Orr-Weaver, T. L. (1994). Double or nothing: a Drosophila mutation affecting meiotic chromosome segregation in both females and males. *Genetics* **136**, 953-964.

Oegema, K., Marshall, W. F., Sedat, J. W. and Alberts, B. M. (1997). Two

proteins that cycle asynchronously between centrosomes and nuclear structures: Drosophila CP60 and CP190. *J. Cell Sci.* **110**, 1573-1583.

Olson, M. O., Dundr, M. and Szebeni, A. (2000). The nucleolus: an old factory with unexpected capabilities. *Trends Cell Biol.* **10**, 189-196.

Paddy, M. R., Saumweber, H., Agard, D. A. and Sedat, J. W. (1996). Time-resolved, in vivo studies of mitotic spindle formation and nuclear lamina breakdown in Drosophila early embryos. *J. Cell Sci.* **109**, 591-607.

Sekelsky, J. J., McKim, K. S., Messina, L., French, R. L., Hurley, W. D., Arbel, T., Chin, G. M., Deneen, B., Force, S. J., Hari, K. L. et al. (1999). Identification of novel Drosophila meiotic genes recovered in a P-element screen. *Genetics* **152**, 529-542.

Spradling, A. (1986). In *Drosophila: A Practical Approach* (ed. D. B. Roberts), pp. 175-197. Oxford, Washington DC: IRL Press.

Sullivan, W., Minden, J. S. and Alberts, B. M. (1990). daughterless-abo-like, a Drosophila maternal-effect mutation that exhibits abnormal centrosome separation during the late blastoderm divisions. *Development* **110**, 311-323.

Theurkauf, W. E. and Hawley, R. S. (1992). Meiotic spindle assembly in Drosophila females: behavior of nonexchange chromosomes and the effects of mutations in the nod kinesin-like protein. *J. Cell Biol.* **116**, 1167-1180.

Tio, M., Zavortink, M., Yang, X. and Chia, W. (1999). A functional analysis of inscuteable and its roles during Drosophila asymmetric cell divisions. *J. Cell Sci.* **112 (Pt 10)**, 1541-1551.

Vazquez, J., Belmont, A. S. and Sedat, J. W. (2001). Multiple regimes of constrained chromosome motion are regulated in the interphase Drosophila nucleus. *Curr. Biol.* **11**, 1227-1239.

Vazquez, J., Belmont, A. and Sedat, J. (2002). The dynamics of homologous chromosome pairing during male Drosophila meiosis. *Curr. Biol.* **12**, 1473-1483.

VijayRaghavan, K., Kaur, J., Paranjape, J. and Rodrigues, V. (1992). The east gene of *Drosophila melanogaster* is expressed in the developing embryonic nervous system and is required for normal olfactory and gustatory responses of the adult. *Dev. Biol.* **154**, 23-36.

Walker, D. L., Wang, D., Jin, Y., Rath, U., Wang, Y. M., Johansen, J. and Johansen, K. M. (2000). Skeletor, a novel chromosomal protein that redistributes during mitosis provides evidence for the formation of a spindle matrix. *J. Cell Biol.* **151**, 1401-1411.

Wasser, M. and Chia, W. (2000). The EAST protein of drosophila controls an expandable nuclear endoskeleton. *Nat. Cell Biol.* **2**, 268-275.

Wei, Y., Mizzen, C. A., Cook, R. G., Gorovsky, M. A. and Allis, C. D. (1998). Phosphorylation of histone H3 at serine 10 is correlated with chromosome condensation during mitosis and meiosis in Tetrahymena. *Proc. Natl. Acad. Sci. USA* **95**, 7480-7484.

Zalokar, M., Audit, C. and Erk, I. (1975). Developmental defects of female-sterile mutants of *Drosophila melanogaster*. *Dev. Biol.* **47**, 419-432.

Zimowska, G., Aris, J. P. and Paddy, M. R. (1997). A Drosophila TPR protein homolog is localized both in the extrachromosomal channel network and to nuclear pore complexes. *J. Cell Sci.* **110**, 927-944.